JOURNAL OF THERMOPHYSICS AND HEAT TRANSFER
Vol. 7, No. 1, Jan.–March 1993

Analytical Comparison of Convective Heat Transfer Correlations in Supercritical Hydrogen

William M. Dziedzic* and Stuart C. Jones†
Lockheed Engineering and Science Company, Hampton, Virginia 23666
and
Dana C. Gould‡ and Dennis H. Petley‡
NASA Langley Research Center, Hampton, Virginia 23681

Four correlations which cover the ranges of liquid to gas for turbulent flow convection of hydrogen were compared with computational fluid dynamics (CFD) analysis over a range of expected design conditions for active cooling of hypersonic aircraft. The correlations compared here are those of Hess and Kunz; McCarthy and Wolf; Miller, Seader, and Trebes; and Taylor. Analysis of hydrogen cooling in a typical cooling panel demonstrated how predicted design performance varies with the correlation used. The Taylor heat transfer coefficient correlation demonstrated the best overall agreement with the CFD results for constant heat flux over a wide range of pressure, temperature, mass flow, and heat load conditions. The McCarthy and Wolf correlation also agreed well with the CFD results. The CFD heat transfer coefficient results for a heat spike differed greatly from all four correlations. An acceptable heat transfer coefficient can be calculated at the heat spike location by ignoring the coefficient at the spike and averaging the coefficient before-and-after the spike. Test data are needed to define the cooling effectiveness of hydrogen for two critical design conditions: 1) a heat spike for all inlet temperatures and pressures; and 2) high heat flux, with low inlet temperature, and high inlet pressure.

Nomenclature

A = area
b = bulk (subscript indicates properties evaluated at bulk temperature T_b)
c_p = specific heat at constant pressure
D = diameter
D_h = hydraulic diameter
dA = differential area
e/D = relative roughness
f = film (subscript indicates properties evaluated at film temperature T_f)
ff = friction factor
k = kinetic energy of turbulence
L = channel length
Nu = Nusselt number
Pr = Prandtl number
R = Rankine
Re = Reynolds number
T = temperature
T_b = bulk temperature
T_s = surface temperature
T_f = reference (subscript indicates properties evaluated at $T_f = T_b + 0.5(T_s - T_b)$
Q = heat rate
u = velocity
u' = local velocity
u_{ave} = average velocity
x = distance from entrance of panel
Δp = pressure drop
ε = dissipation rate of turbulence
ν = kinematic viscosity
ρ = density
∞ = infinity
0.4 = reference (subscript indicates properties evaluated at $T_{0.4} = T_b + 0.4(T_s - T_b)$

Introduction

HYDROGEN fuel is currently used in the Space Shuttle and has been proposed for use in hypersonic aircraft such as the National Aerospace Plane (NASP). Active cooling is necessary for scramjet engines to survive the extreme heat generated in hypersonic flight and hydrogen fuel will be used as the coolant. Cooling system performance is a strong function of the rate of convective heat transfer from the hot walls of the cooling panels to the hydrogen. Several empirical correlating equations have been developed and are in use to calculate the convective heat transfer coefficient. When applied to cryogenic hydrogen in the high-heat-flux, high-pressure regions of some designs these equations often give widely different heat transfer coefficients. This raises the question of which, if any, of these equations are applicable to these designs. Unfortunately no experimental test data are available in these regions.

Background

There are many correlations for predicting single-phase heat transfer coefficients for turbulent flow of hydrogen in tubes. The bulk of these correlations were developed in the mid-to-late 1960s. Since this time little has been published on this subject. The majority of these correlations have limited ranges of applicability due to large variations in the physical properties of hydrogen. Worse yet, there are important states of hydrogen where no correlations apply. (The kinematic viscosity of para-hydrogen is shown in Fig. 1.) The fluid properties of hydrogen such as kinematic viscosity can be separated into two regions: 1) liquid-like, and 2) gas-like. In the liquid region viscosity decreases as the temperature increases; in the

Received May 31, 1991; presented as Paper 91-1382 at the AIAA 26th Thermophysics Conference, Honolulu, HI, June 24–26, 1991; revision received Jan. 30, 1992; accepted for publication Jan. 31, 1992.

*Senior Aerospace Engineer, Langley Program Office, 144 Research Drive, MS 350.
†Research Engineer, General Electric Medical Systems, Cyostat Engineering, P.O. Box 100539, Florence, SC.
‡Aerospace Technologist, NASPO/SAO, MS 350.

Table 1 Summary of ranges for heat transfer correlations of supercritical hydrogen

Parameter	Hess and Kunz	McCarthy and Wolf	Miller, Seader, and Trebes	Taylor
X/D	——	6–50	5–47	2–252
T_s/T_b	3–14	2–11	2–28	1–23
T_{inlet}, °R	57–120	135–560	51–69	45–180
Press, psi	235–745	32–1354	458–2486	531–2500
Heat flux, Btu/s-ft^2	88–1463	5–2131	197–3456	5–3974
Mass flow rate, lb/s	——	0.001–0.13	0.2–0.7	——
T_s, °R	——	830–2240	107–1730	14–5630
ID, in.	0.2–0.3	0.2–0.4	0.2	——

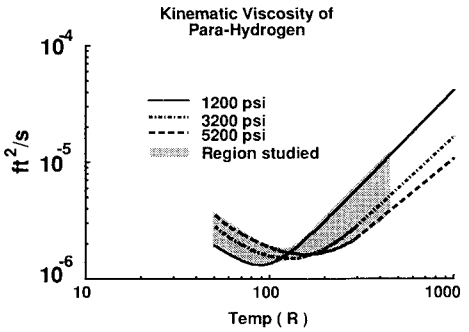

Fig. 1 Kinematic viscosity of para-hydrogen.

gas region viscosity increases as the temperature increases. The transition occurs within a broad band of temperature and pressure. The correlations have a difficult time predicting heat transfer coefficients when the hydrogen passes from the liquid region to the gas region. This study examined three heat transfer correlations which are used throughout the aerospace industry and one which has been proposed to cover a relatively wide range of flow conditions in a single correlation.

The first correlation was developed by H. L. Hess and H. R. Kunz.[1] This correlation uses a kinematic viscosity ratio. The recommended range of applicability is shown in Table 1. This correlation gives reasonable results (within 25%) for low temperature and low pressure hydrogen (liquid region):

$$Nu_f = 0.0208 Re_f^{0.8} Pr_f^{0.4}(1 + 0.01457 \nu_s/\nu_b) \quad (1)$$

The second correlation was developed by J. R. McCarthy and H. L. Wolf.[2] This correlation uses a surface to bulk temperature ratio. The recommended range of applicability is shown in Table 1. This correlation gives reasonable results (within 25%) for high temperature and low pressure hydrogen (gas region):

$$Nu_b = 0.025 Re_b^{0.8} Pr_b^{0.4}(T_s/T_b)^{-0.55} \quad (2)$$

The third correlation was developed by W. S. Miller et al.[3] and also uses a kinematic viscosity ratio. The recommended range of applicability is shown in Table 1. This correlation gives reasonable results (within 25%) for low temperature and high pressure hydrogen (liquid region):

$$Nu_{0.4} = 0.0208(Re_{0.4})^{0.8}(Pr_{0.4})^{0.4}(1 + 0.00983 \nu_s/\nu_b) \quad (3)$$

The fourth and last correlation studied was developed by M. F. Taylor.[4] This equation uses the surface to bulk temperature ratio and is also the only one of the four correlations that includes entrance effects. The recommended range of applicability is shown in Table 1. This correlation gives reasonable results (within 25%) for a relatively wide temperature and pressure range of hydrogen:

$$Nu_b = 0.023 Re_b^{0.8} Pr_b^{0.4}(T_s/T_b)^{-(0.57-1.59D/X)} \quad (4)$$

Methods

The test geometry was a 10-in. (25.4-cm) long cooling channel. The hydrogen flow Mach numbers were as high as 0.34 with supply pressures between 1000–5000 psi (6.9–34.5 MPa). The range of supply temperatures were from 50–500°R (28–278 K). The NASP/SINDA[5,6] thermal management code was used for the system analysis using heat transfer coefficients based on the correlations. The FLUENT[7] code was used for the computational fluid dynamics (CFD) analysis. Results of the engineering method using the correlations were compared with the results of the CFD analysis for several regions of temperature and pressure.

The purpose of this article is to demonstrate how predicted cooling panel performance varies with each correlation for different sets of design conditions. Due to the lack of test data, CFD analysis was used for comparison. Results are presented for each correlation relative to the CFD results. Analytical results from both NASP/SINDA and FLUENT have compared well with other established fluid and heat transfer programs. The FLUENT results are expected to be within 20% for the constant heat flux results. The heat spike results may not be within 20%.

The NASP/SINDA program was written to analyze entire cooling systems for hypersonic aircraft, including conduction and convection in cooling panels. NASP/SINDA is a customized version of the finite difference, heat transfer computer program SINDA '85.[8] FORTRAN subroutines have been written into the program to calculate pressure drop for one-dimensional flow down the length of a cooling panel pipe or duct using the boundary-layer assumptions. Pressure drop calculations are based on a compressible flow equation with friction and heat addition.[9] Moody friction factors[10] were calculated by Eq. (5):

$$1/ff^{0.5} = 2 \log_{10}\left(\frac{e/D}{3.7} + \frac{2.5}{Re_D ff^{0.5}}\right) \quad (5)$$

Conduction of heat through the walls of the cooling panel are calculated using the finite difference solution subroutines in Sinda '85. Any heat transfer convection correlation can be input into the program and used to predict the heat transfer coefficient from the cooling panel walls to the fluid. A data base called GASPLUS,[11] developed at NASA Lewis Research Center, was used for the fluid properties.

FLUENT is a general purpose computer program for modeling internal and external fluid flows. FLUENT performs finite difference solutions of the Navier-Stokes equations along with conservation of the parameters in the k-ε turbulence model.[7] The model uses temperature dependent hydrogen properties based on the GASPLUS software for consistency with NASP/SINDA. Properties are evaluated at the average pressure.

Four correlations for turbulent flow convection of hydrogen were compared with CFD analysis over a range of expected design conditions for active cooling of hypersonic aircraft. Coolant channels with two different types of heat flux distributions were studied, a constant heat flux and a heat spike. Heat spikes will occur at locations of impinging shocks. These

Table 2a Temperature, pressure, and heat flux matrix (for a straight 0.05-in. hydraulic diameter channel, constant heat flux)

Inlet total temperature, °R	Inlet static press, psi	Heat flux,[a] Btu/ft²-s
50	1000	100
150	2000	1000
200	5000	2500
500	—	3500

[a]All 48 possible combinations of temperature, pressure, and heat flux were investigated for each correlation.

Table 2b Temperature, pressure, and heat flux matrix (for a straight 0.05-in. hydraulic diameter channel, with a heat spike)

Inlet total temperature, °R	Inlet static press, psi	Heat spike,[a] Btu/ft²-s
50	1000	5000
150	2000	—
200	5000	—
500	—	—

[a]All 12 possible combinations of temperature and pressure for the given heat spike were investigated for each correlation.

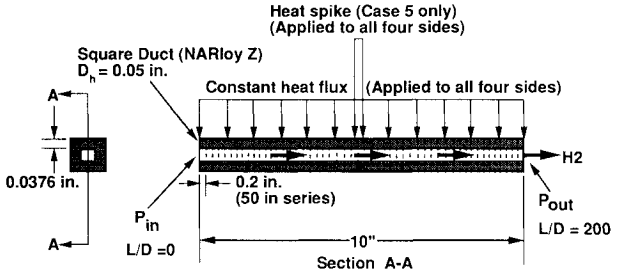

Fig. 2 Cooling panel test case.

coolant channels closely resemble channels which would be used for the NASP. A matrix of varying inlet temperatures, pressures and heat fluxes was examined (see Tables 2a and 2b).

The constant area, constant heat flux channel is shown in Fig. 2. The channel has a hydraulic diameter of 0.05 in. (0.127 cm), a flow area of 0.0025 in.² (0.0161 cm²) and an overall length of 10 in. (25.4 cm). Within NASP/SINDA the 10-in. (25.4-cm) channel was modeled as 50 0.2-in. (0.508-cm) long panels arranged in series. The thickness of the heated wall was 0.0376 in. (0.0955 cm) and the thickness of the inner wall was 0.08 in. (0.20 cm). The land thickness was 0.0444 in. (0.1128 cm). The channel walls were assumed to be smooth.

A heat spike was applied to the midpoint of the 10-in. (25.4-cm) long channel as shown in Fig. 2. The heat spike was 0.4-in. (1.0-cm) long, the area before and after the spike had a constant heat flux of 500 Btu/(ft²-s). The channel dimensions were the same as those used in the constant heat flux analysis.

There were a total of 48 possible combinations of temperature, pressure, and heat flux for a straight constant area, constant heat flux channel. All 48 NASP/SINDA runs were made using each of the four correlations. There were also 12 possible combinations of temperature and pressure for a straight constant area channel with a heat spike. All 12 NASP/SINDA heat spike runs were used for each of the four correlations. The Taylor equation is the only one of the four that includes entrance effects. When the other three correlations were used, a correction factor was applied to represent entrance effects shown in Fig. 3. Results of the 60 NASP/SINDA runs were studied and five were chosen to be analyzed with CFD.

The FLUENT model consisted of flow in a 0.05-in (0.127-cm) diameter pipe 10-in. (25.4-cm) long. Inlet turbulence in-

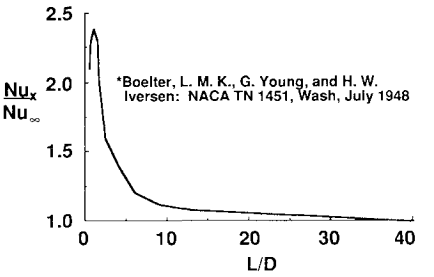

Fig. 3 Combined hydrodynamic and thermal entry length in a circular tube.*

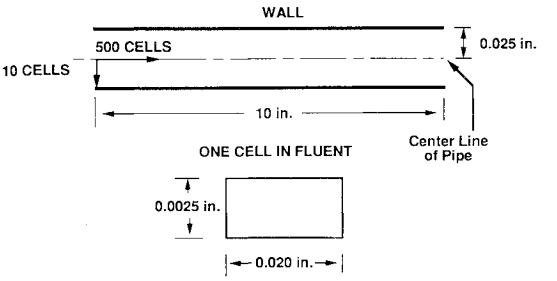

Fig. 4 FLUENT axisymmetric numerical grid.

tensity was set to 5% at the inlet ($u'/u_{ave} = 0.05$). The numerical grid was 500 cells axially (width) and 10 cells radially between the wall and the symmetry boundary (height) as shown in Fig. 4. This grid was chosen based on the desire for a reasonable aspect ratio (a recommendation of $AR = 8$ was made by the code developers) while using the code limit of 500 cells in any given direction. A grid sensitivity study was performed for case 1 only. Also, the code used a log-law wall function which implies a dimensionless distance from the wall y_p^+ greater than 25 for the first grid point.[7] The heat transfer coefficient, bulk temperature, and friction factor were determined by Eqs. (6–8):

$$h = \frac{Q}{(Tw - Tb)} \tag{6}$$

$$T_b = \frac{\int (\rho u c_p T)\, dA}{\int (\rho u c_p)\, dA} \tag{7}$$

$$ff = \frac{\Delta p D}{0.5 \rho u^2 L} \tag{8}$$

Several cases were run using a finer grid on a shorter pipe with the answers indicating the chosen grid to be sufficient.

The CFD results were then compared with the NASP/SINDA results. This comparison was obtained by matching the mass flow rate, inlet temperature, inlet pressure, and heat flux. The wall and land dimensions were changed in the NASP/SINDA channel model for the comparison of results between NASP/SINDA and FLUENT. The top and bottom wall thickness and land thickness were decreased to 0.0188 in. The flow area was not changed. Heat was applied to the outside wall of the NASP/SINDA channel model, the FLUENT pipe flow model had zero thickness walls, therefore, the heat was applied directly to the fluid. The heat flux was adjusted by the ratio of the circumferences (0.448) as shown in Eq. (9):

$$Q_{square}/Q_{pipe} = \frac{(\pi D)}{4(\text{width} + \text{land thickness})} \tag{9}$$

The NASP/SINDA analysis assumed two-dimensional conduction. Asymmetric heating[12] and three-dimensional conduction were analyzed and determined not to be important

factors in comparisons between analyses using the four correlations. Five cases representing five cooling panel design conditions were chosen for CFD analysis and comparison with the heat transfer correlations as used in NASP/SINDA. Case 1 was used as a validation case for the CFD model because of the excellent agreement between all four correlations across the entire channel length. This case, with a high inlet temperature, high inlet pressure and low constant heat flux, represents the gas region of the hydrogen fluid properties. Case 2 with low inlet temperature, high inlet pressure, and high constant heat flux represents the liquid region near the entrance, with transition to the gas region. Case 3 with low inlet temperature, moderate inlet pressure, and low constant heat flux, represents the liquid region. Case 4 is at low inlet temperature, high inlet pressure, and low constant heat flux. The fluid in this case cannot be described as a liquid or as a gas. Case 5 is at low inlet temperature and high inlet pressure with a heat spike at the center of the channel. These conditions represent the liquid region of the hydrogen fluid properties.

Results

The results of case 1 are shown in Fig. 5. Excellent agreement was obtained between the four correlations and FLUENT for the entire channel length with the exception of the entrance region. This case represents high pressure, high temperature, and low heat flux design conditions. The hydrogen acts more as a gas in this region. These conditions fall outside the recommended ranges of inlet pressure and inlet temperature for Miller, Seader and Trebes, and Hess and Kunz, and inlet pressure for Taylor and McCarthy and Wolf. Taylor's entrance effect agreed with FLUENT's entrance effect, while the entrance effect table factor used with the other three equations did not agree well. This was true for all cases. It was also observed that varying the inlet pressure between 1000–5000 psi (6.9–34.5 MPa) while holding the inlet temperature and heat flux constant, had very little effect on the results.

Case 2, shown in Fig. 6, offers the widest variation in heat transfer coefficients between the four correlations and the CFD analysis for the constant heat flux. This case represents a high heat flux, high pressure, and low inlet temperature cooling panel. The hydrogen starts out in the liquid region but quickly heats up into the gas region. These conditions fall outside the recommended ranges of inlet pressure for Miller, Seader and Trebes, Hess and Kunz, and Taylor and inlet pressure and inlet temperature for McCarthy and Wolf. The Hess and Kunz, and Miller, Seader and Trebes correlations, which are based on the kinematic viscosity ratio, agreed with each other but differed from the CFD results by as much as 17% at the exit and over 100% near the entrance. The Taylor and McCarthy and Wolf correlations, which are based on surface to bulk temperature ratio, are in relatively close agreement with the CFD results. The closest agreement with the CFD results of the four correlations was Taylor which differed by 7% at the exit and a maximum deviation of 24% along the length. The four correlations appeared to be converging to the same coefficient at the exit of this channel. The results of other NASP/SINDA runs indicated that increasing the inlet temperature from 50 to 500°R (28–278 K) reduced the differences in heat transfer coefficient between the correlations. Other runs also indicated reducing the inlet pressure from 5000 to 1000 psi (34.5–6.9 MPa) reduces the differences in heat transfer coefficients between correlations. This is due to the effect of high inlet pressure, low inlet temperature, and high heat flux on viscosity. At a given temperature above 103°R (57.2 K), the kinematic viscosity of hydrogen is lower and varies less with temperature in the liquid region at 5000 psi (34.5 MPa) than at 1000 psi (6.9 MPa) (see Fig. 1). The viscosity ratio correlations are much more sensitive to viscosity changes due to temperature and pressure than are the temperature ratio correlations. The fluid temperature at the surface increases much faster than the bulk temperature. Therefore, the fluid properties at the surface are in the gas region while the bulk fluid properties remain in the liquid region. This causes the viscosity ratio correlations to predict a higher heat transfer coefficient than the temperature ratio correlations.

The results of case 3 shown in Fig. 7 represent conditions where the hydrogen acts as a liquid throughout the panel length. This case has moderate inlet pressure, low inlet temperature, and low heat flux. These conditions fall outside the

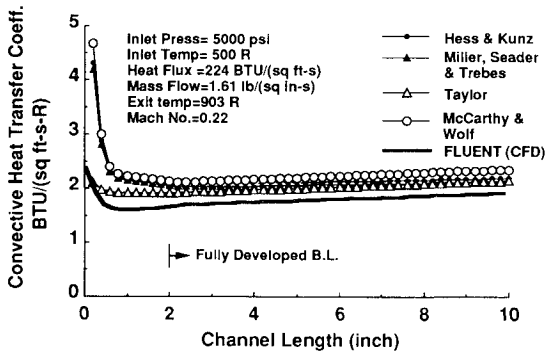

Fig. 5 Case 1, baseline.

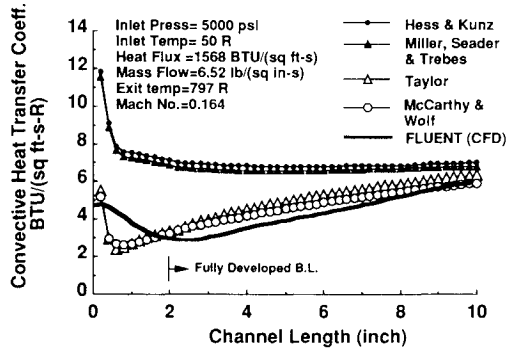

Fig. 6 Case 2, gas region.

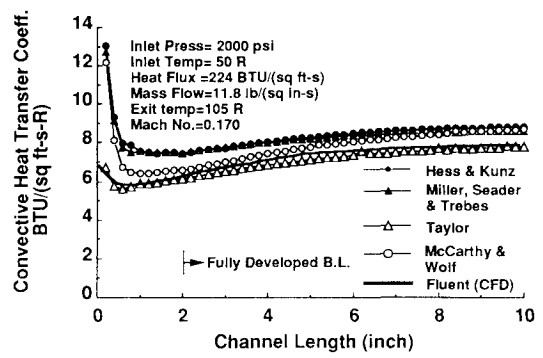

Fig. 7 Case 3, liquid region.

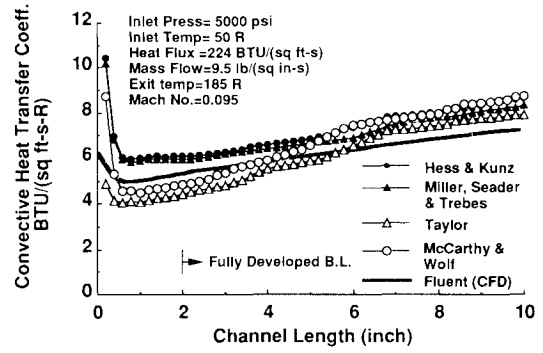

Fig. 8 Case 4, transition region.

recommended range of inlet temperature and inlet pressure for McCarthy and Wolf and inlet pressure for Hess and Kunz. The Taylor results agreed within 2% of the CFD results at the exit and 9% near the entrance.

The results of case 4 shown in Fig. 8 represent conditions nearly identical to case 3 except that the inlet pressure was increased from 2000 to 5000 psi (13.8–34.5 MPa). These conditions fall outside the recommended range of inlet temperature and inlet pressure for McCarthy and Wolf and inlet pressure for Hess and Kunz; Miller, Seader and Trebes; and Taylor. The Taylor heat transfer coefficient results are now within 8% of the CFD results at the exit and 35% near the entrance.

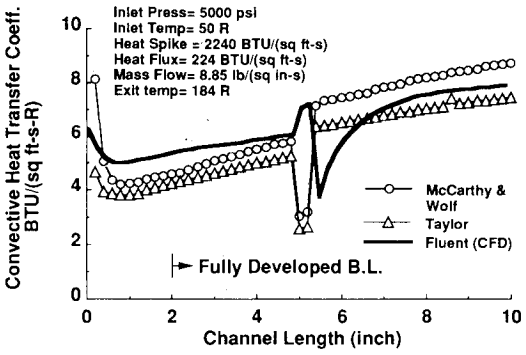

Fig. 9a Case 5, heat spike results for temperature ratio correlations.

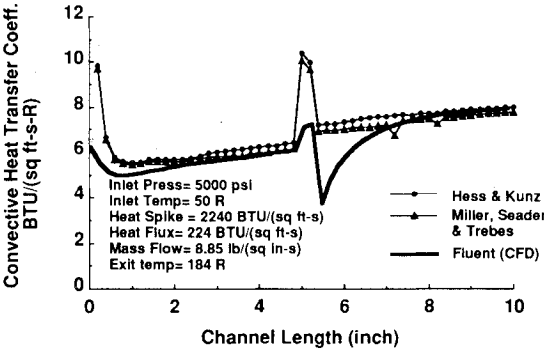

Fig. 9b Case 5, heat spike results for viscosity ratio correlations.

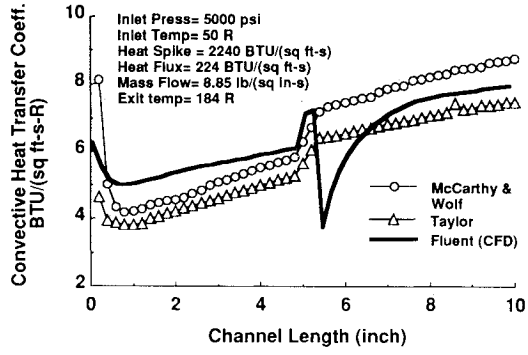

Fig. 9c Case 5, averaging method at the heat spike.

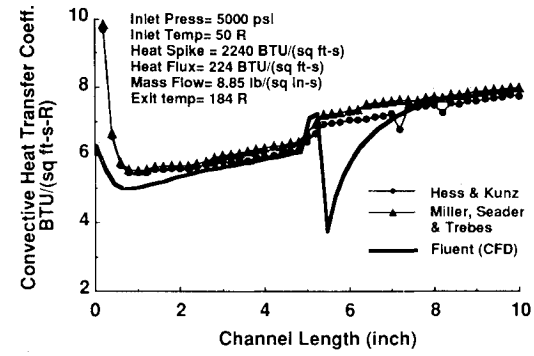

Fig. 9d Case 5, averaging method at the heat spike.

Case 5 shown in Figs. 9a and 9b demonstrates the effect of a heat spike on the four heat transfer coefficient correlations. A thermal entry factor was used for the heat transfer coefficient at the spike for all four correlations. The correlations were not tested for heat spike conditions and were not expected to be accurate. Miller, Seader and Trebes, and Hess and Kunz showed a significant increase in heat transfer coefficient where the heat spike was applied, whereas, Taylor, and McCarthy and Wolf show a significant decrease. The CFD results demonstrated a slight increase at the point of the spike and a significant decrease immediately after the spike. The inlet pressure, temperature, and heat flux were varied, but the trend was basically the same. The liquid-gas region viscosity effect for the bulk and surface fluid temperature causes the viscosity ratio correlations to predict relatively high heat transfer correlations at the heat spike. The high surface to bulk temperature ratio at the heat spike causes the temperature ratio correlations to predict relatively low heat transfer coefficients.

The analysis of a heat spike is critical for the cooling panel design selection of materials, wall thicknesses and hydrogen mass flow rates for proper cooling. Currently there is no heat transfer coefficient correlation which accurately predicts how the heat is transferred into the fluid for a heat spike. Based on the results of this article the following engineering solution is recommended until further analysis can be completed. An acceptable heat transfer coefficient can be calculated at the heat spike location by ignoring the coefficient at the spike and averaging the coefficient before-and-after the spike as shown in Figs. 9c and 9d. This method works for the spike location but immediately after the spike the CFD results indicate a relatively large decrease in the heat transfer coefficient. Downstream of the spike the fluid near the wall is very hot while the bulk temperature has only increased slightly at this location. The high temperature fluid in the turbulent boundary layer, which is near the wall, causes the wall temperature to be high even though the heat rate is low. This causes a very low heat transfer coefficient. The rapid recovery of heat transfer is due to a decrease in the boundary layer temperature as the fluid in the core and boundary layer continue to mix. This effect can be seen as an inverse thermal entrance effect. The correlations do not predict the drop in heat transfer coefficient due to their dependence on the bulk temperature only. Downstream of the spike the effect on wall temperature is small if the heat rate is small and may not be important in many designs.

Friction factors and Reynolds numbers based on bulk temperature for cases 4 and 5 are compared in Figs. 10 and 11. Case 4 was the low heat flux, high inlet pressure, and low inlet temperature. Case 5 was the heat spike model with low inlet temperature and high inlet pressure. The friction factors calculated by Moody are within 30% of those calculated by CFD for case 4. The CFD friction factor in case 5 shows a large increase at the location of the heat spike while the Moody

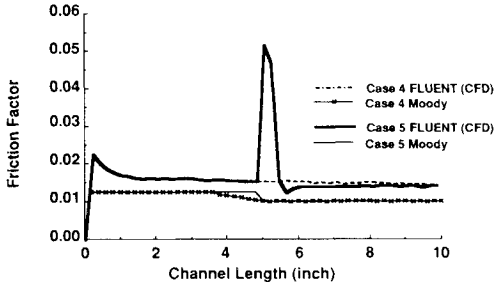

Fig. 10 Comparison of friction factor correlations with CFD.

Table 3 Summary of parameters for cases 1–5

Case no.	Vel., ft/s	Film *Re*, $\times 10^5$	*Pr*	Press drop, psi
1	432–571	4.1–3.5	0.64–0.63	105
2	243–1145	7.1–3.7	0.71–0.61	334
3	63–573	11.0–19.0	0.96–0.77	334
4	246–421	6.1–10.0	0.98–0.77	186
5	250–451	6.4–10.9	0.98–0.77	186

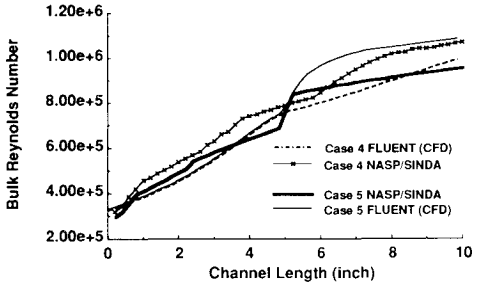

Fig. 11 Comparison of bulk Reynolds number with CFD.

friction factor remains constant. The difference in friction factors between NASP/SINDA and CFD for case 5 excluding the spike was a maximum 35%. Further study is needed in this area. The Reynolds number based on bulk temperature is displayed in Fig. 11. The Reynolds numbers calculated by NASP/SINDA were within 14% of those calculated by CFD for case 4 and 16% for case 5. Table 3 summarizes the ranges of velocity, film Reynolds number, Prandtl number, and pressure drop for all five cases.

This article has highlighted the need for testing of hydrogen cooled panels. Test data are needed to define the cooling effectiveness of hydrogen for two critical design conditions: 1) a heat spike condition; and 2) the low inlet temperature, high heat flux, and high pressure condition.

Conclusions

1. The Taylor heat transfer coefficient correlation demonstrated the best overall agreement with the CFD results for constant heat flux over a wide range of pressure, temperature, mass flow, and heat flux conditions.

2. The Taylor correlation predictions for entrance effects also agreed well with the CFD results.

3. The CFD heat transfer coefficient results for a heat spike differed greatly from all four correlations.

4. An acceptable heat transfer coefficient can be calculated at the heat spike location by ignoring the coefficient at the spike and averaging the coefficient before-and-after the spike.

5. Test data are needed to define the cooling effectiveness of hydrogen for two critical design conditions: 1) a heat spike for all inlet temperatures and pressures; and 2) for a high heat flux with low inlet temperature, and high pressure.

Acknowledgments

The authors express their thanks to Liz Marshall of Creare.X Corp. and Pradeep Kamath of Analytical Services & Materials, Inc. for their help with the CFD analysis.

References

[1]Hess, H. L., and Kunz, H. R., "A Study of Forced Convection Heat Transfer to Supercritical Hydrogen," *Journal of Heat Transfer*, Vol. 87, No. 1, 1965, pp. 41–48.

[2]McCarthy, J. R., and Wolf, H., "The Heat Transfer Characteristics of Gaseous Hydrogen and Helium," Rocketdyne Div., North American Aviation, Rept. R-60-12, Canoga Park, CA, Dec. 1960.

[3]Miller, W. S., Seader, J. D., and Trebes, D. M., "Forced Convection Heat Transfer to Liquid Hydrogen at Super-Critical Pressures," *Pure and Applied Cryogenics*, Vol. 4, Sec. IV, June 1965, pp. 173–191.

[4]Taylor, M. F., "Correlation of Local Heat-Transfer Coefficients for Single-Phase Turbulent Flow of Hydrogen in Tubes with Temperature Ratios to 23," NASA TN D-4332, Jan. 1968.

[5]Petley, D. H., Jones, S. C., and Dziedzic, W. M., "Analysis of Cooling Systems for Hypersonic Aircraft," Third International Aerospace Planes Conf., AIAA Paper 91-5063, Orlando, FL, Dec. 1991.

[6]Petley, D. H., Jones, S. C., and Dziedzic, W. M., "Integrated Numerical Methods for Hypersonic Aircraft Cooling Systems Analysis," 30th Aerospace Sciences Meeting & Exhibit, AIAA Paper 92-0254, Reno, NV, Jan. 1992.

[7]Anon., "FLUENT Users Manual," Creare.X Corp., Hanover, NH, March 1990.

[8]Anon., "SINDA '85/FLUINT User's Manual," Denver Aerospace Div. of Martin Marietta, Denver, CO, Nov. 1987.

[9]John, J. E. A., *Gas Dynamics*, Allen and Beacon, Boston, MA, 1969.

[10]Parker, J. D., Boggs, J. H., and Blick, E. F., *Introduction to Fluid Mechanics and Heat Transfer*, Addison-Wesley, Reading, MA, 1969.

[11]Fowler, J. R., GASPLUS User's Manual (Preliminary NASP Copy), NASA Lewis Research Center, Cleveland, OH, Aug. 1988.

[12]Anon., "Investigation of Cooling Problems at High Chamber Pressures Final Report." Rocketdyne-North American Aviation, Rept. R-6529, Canoga Park, CA, Sept. 1966.